J Mater Sci (2007) 42:828–833
DOI 10.1007/s10853-006-0080-1

Effect of lithium additive on the microstructure and electrical responses of 0.9PMN–0.1PT ceramics

Alberto Adriano Cavalheiro · Juliana C. Bruno · Maria A. Zaghete · José A. Varela

Received: 10 April 2005 / Accepted: 29 March 2006 / Published online: 11 January 2007

Abstract Structural effects of lithium additive on 0.9PMN–0.1PT powders prepared by Ti-modified columbite route were studied. The substitution of Li^+ ions for Mg^{2+} ions in the B-site sub-lattice of 0.9PMN–0.1PT perovskite structure was explained in terms of lead and oxygen vacancies generation originated as consequence of the ionic compensation of negatively charged Li'_{Mg} sites. The rise in mass transport as consequence of the increasing of Pb^{2+} and O^{2-} vacancies produces more agglomerated particles during the powder synthesis and changes the mechanical characteristics between grain and grain boundary of sintered ceramic. The relation between K_m and T_m values, the difference between ionic radii of B cation and the molar volume were used to explain the changes in the relaxor behavior and diffusiveness of phase transition as function of lithium doping, which are corroborated by the results obtained through the ferroelectric characterization.

A. A. Cavalheiro (✉)
Depto de Química, Instituto de Biociências – UNESP, Distrito de Rubião Junior, s/n, Zip Code 18.618-000
P.O. Box 510, Botucatu, SP, Brazil
e-mail: albecava@bol.com.br

J. C. Bruno · M. A. Zaghete · J. A. Varela
Liec – Instituto de Química – UNESP, Rua Prof. Francisco Degni, s/n, Zip Code 14.801-970, P.O. Box 355, Araraquara, SP, Brazil

Introduction

Lead based perovskite structures have drawn attention during last years owing to their industrial applications such as multilayer capacitors, electro-mechanical coupling devices and actuators [1–5]. The relaxor ferroelectric ceramic $0.9Pb(Mg_{1/3}Nb_{2/3})O_3$–$0.1PbTiO_3$ is an interesting composition because the addition of 10 mol% of titanium displaces T_m to room temperature. Furthermore, PMN–PT actuator materials can exhibit excellent machinability and high dielectric and mechanical strengths [6].

From the viewpoint of preparation methods, the properties of Pb-based ceramics can be affected by several synthesis parameters. It is very difficult to obtain single-phase perovskite PMN via conventional oxide mixture due to the formation of pyrochlore phase [7]. However, by using the columbite route [8] the preferential reaction between lead and niobium oxides can be avoided, making feasible to get large amount of perovskite phase in PMN powder. Besides, the addition of $PbTiO_3$ in PMN system can also reduce the amount of pyrochlore phase, once titanium in B site stabilizes perovskite phase by avoiding PbO volatilization [9]. Compositions of $(1 - x)$PMN–xPT can be synthesized using the columbite route but the individual synthesis of titanium precursor component makes difficult to keep reproducible in all fabrication stages, concerning powder surface reactivity, chemical homogeneity, and its consequences on the synthesis conditions for the phase formation [10].

Taking in account these difficulties, we have proposed recently the synthesis of PMN–PT powders adapting the traditional columbite route. This new methodology is based on the preparation of the

Ti-modified columbite precursor. Using the polymeric precursor method, chemically homogeneous MN_T precursor can be prepared at lower temperature such as 900 °C [11]. The high surface reactivity of the obtained precursor allows synthesizing pyrochlore-free PMN–PT powders by solid state reaction with PbO at 800 °C. Based in recent work [12], where was demonstrated that lithium additive in PMN ceramics acts favorably on the sintering stage and dielectric properties, we proposed to study the effect of lithium additive during the entire synthesis process of the PMN–PT ceramic via Ti-modified columbite route. Initial results about phase formation and structural changes in MN_T precursor in the additive presence were already published [11], and the present work will report its consequences on electrical properties.

Experimental procedure

The 0.9PMN–0.1PT powders were prepared using the Ti-modified columbite precursor method, and the details of processing were described earlier [11]. The starting materials for MN_T precursor synthesis are analytically pure: Nb_2O_5, $(MgCO_3)_4{\cdot}Mg(OH)_2{\cdot}5H_2O$, $Ti(OC_3H_7)_4$, and Li_2CO_3. Three different MN_T precursor samples were prepared: no-doped, doped with 1 and 2 mol% of lithium. The final powders were mixed with stoichiometric amount of PbO, homogenized and heat-treated at 800 °C for 2 h to obtain the perovskite PMN–PT powders. A polyacrylate binder was added in the powder samples to improve the compacting process. Pellets with diameter of 1.2 cm were obtained by uniaxial pressing at 50 MPa and the binder was burned out at 500 °C for 1 h prior to sintering. The green bodies were sintered in a sealed system at 1,100 °C for 4 h.

The powder samples and the sintered ceramics were monitored by X-ray diffraction technique (XRD) and the obtained data were used to perform the structure refinement by the Rietveld Method. The microstructure of 0.9PMN–0.1PT powders and the fractured pellets was observed by means of scanning electron microscopy (SEM). Silver electrode was applied on both sides of ceramic samples (12–14 mm of thickness and 1.0–1.1 cm of diameter) before the electrical characterization. Measurements of the capacitance and dielectric loss as function of temperature were got at 1–100 kHz using an HP 4192A impedance analyzer, and the polarization (P) vs. electric-field (E) curves were got at room temperature, using a high tension Radiant equipped with RT600HVS high voltage test system (1.5 kV at 250 Hz).

Results and discussion

The MN_T precursors were characterized by XRD and, as demonstrated in previous works [11, 13], titanium was inserted into the columbite precursor without forming a secondary phase. Besides, for lithium 2 mol%-doped sample, there is the appearance of an extra phase, identified as $LiNbO_3$ rhombohedral phase. Such phase is consequence of the solubility limit for lithium dissolution in MN_T structure, which seems to situate between 1 and 2 mol%. Other structural effects caused by lithium additive in the columbite structure are also presented in the last two mentioned works. For example, the increasing of MN_T powders crystallinity even for 1 mol% of lithium, characterized by a peak rising at 25.2°, and an increasing of the structural ordering, verified by the anisotropic reduction in the unit cell volume due to decreasing in the c parameter.

XRD patterns for 0.9PMN–0.1PT powder samples obtained after solid state reaction between MN_T precursors and stoichiometric amount of PbO at 800 °C for 2 h are shown in Fig. 1. It is possible to observe that only the sample containing 2 mol% of lithium (PL2 sample) (Fig. 1c) presents small amount of secondary phase (*). The possibilities are restricted at few phases of the Pb–Mg–Nb–Ti–Li–O system available in M PDF4 data bank and the most probable is the orthorhombic PbO_2 phase (M PDF: 52-752). Probably, Li (0.76 Å) substitutes Mg (0.72 Å) in the perovskite B site sub-lattice because Nb (0.64 Å) or Ti (0.605 Å) are very small cations to tolerate such substitution, according to the ionic radii values considering the coordination number of VI [14]. In addition, if B cation is substituted by bigger and heterovalent cations in the perovskite structure, then an enlargement in BO_6 octahedron intrinsic distortion can occur.

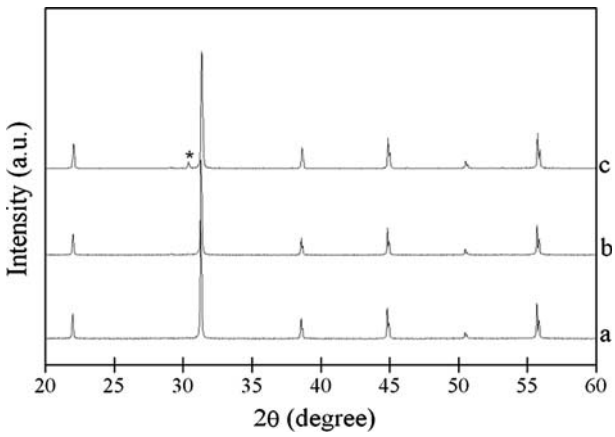

Fig. 1 X-ray diffraction pattern of calcined 0.9PMN–0.1PT powders (**a**) pure, (**b**) PL1, and (**c**) PL2 samples

This event could be verified through the data of the structural refinement (Table 1).

By considering the results of Fanning et al. [15], Mg ion causes oxygen displacement because O–Mg–O bond length (4.14 Å) is not supported by lattice parameter of 4.039 Å. In Table 1 is observed that the oxygen displacement is attenuated when 1 mol% of Li is added to B′ site, due to the decreasing of x coordinate for oxygen from 0.6174 (Pure) to 0.5846 (PL1), besides the increasing in lattice parameter (4.040 Å). Another consequence for lithium substitution is the generation of negatively charged Li'_{Mg} sites [16], which imply in the generation of oxygen vacancies toward the ionic compensation. This compensation can be only obtained if a vacancy of Pb is generated for each two oxygen vacancies leading to PbO_2 segregation. However, for 1 mol% of Li it seems that Pb and O vacancies are very close to the intrinsic Pb deficiency supported by PMN–PT perovskite structure, as reported by Che and Yao [17], so that the extra peak related to any form of lead oxide is not observed in XRD pattern.

For 2 mol% of lithium, the valence and size mismatch originated from the difference in the charge and size between Li^+ and Mg^{2+} cations localized in B′-random site becomes greater and an expected increasing in constant cell is compensated by more Pb deficiency, making it to stay unaltered (4.040 Å) if compared to 1 mol% of Li. Thus, more amounts of vacancies of Pb and O are necessary to reach the charge compensation, which causes a significant PbO_2 segregation in order to exhibit a characteristic peak in XRD pattern for PL2 sample. This result contradicts previous conclusions about the perovskite degradation when 2 mol% of potassium is added to 0.9PMN–PT system [18]. A revision of mentioned results showed that, different from Li doping, the PbO_2 phase is segregated by a direct generation of Pb vacancies when K substitutes Pb in the A site of perovskite structure. In addition, PbO_2 orthorhombic phase seems to be a metastable phase once in sintered ceramics it is not identified.

Table 1 Data of perovskite lattice parameter and x coordinates for B cation and oxygen in ABO_3 structure

Sample	Lattice parameter (Å)	x coordinates (SGR: P m^{-3} m)*		Δx
		B cation (x, ½, ½)	Oxygen (x, ½, 0)	
Pure	4.039	0.5441	0.6174	0.0733
PL1	4.040	0.4479	0.5846	0.1367
PL2	4.040	0.4599	0.5702	0.1103

* ICSD collection code: 72226

Figure 2 shows the SEM images for 0.9PMN–0.1PT powder samples. The main feature of this system is particles close to 1.0 μm in size, independent of lithium presence. Nevertheless, when lithium is added (Fig. 2b, c) the agglomerate degree tends to increase significantly. For PL1 sample, the agglomeration degree is less accentuated than PL2, due to the significant

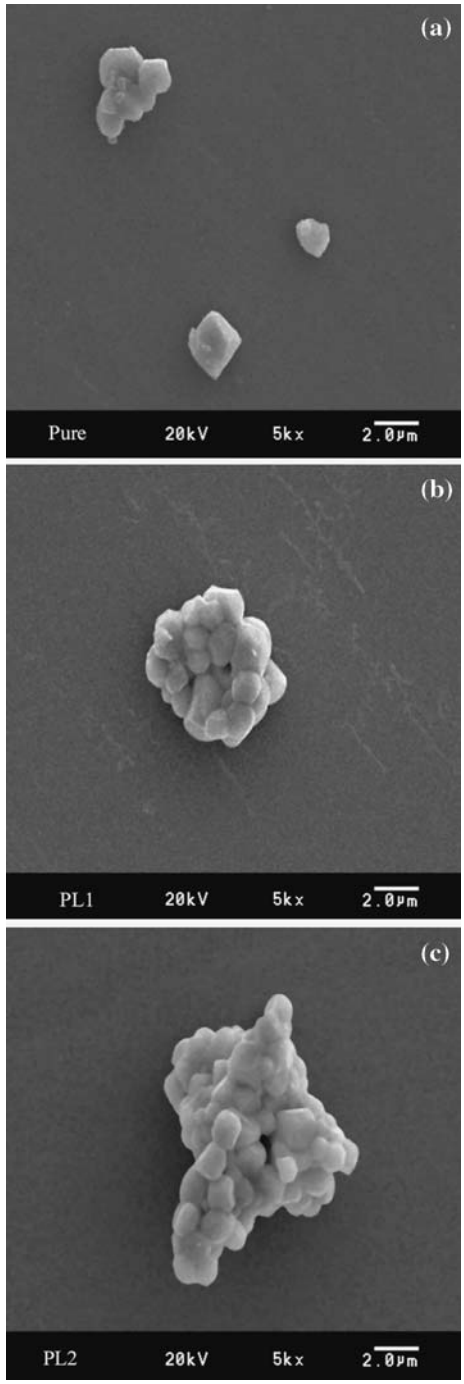

Fig. 2 SEM images of 0.9PMN–0.1PT powders (**a**) pure, (**b**) PL1, and (**c**) PL2 samples

amount of PbO_2 segregated for PL2 sample besides the increasing in the concentration of vacancies, which implies in an increasing in mass transport, leading to more agglomerated powders.

The obtained data after the sintering process for the ceramic samples had shown that doped samples exhibit minor weight loss compared to pure 0.9PMN–0.1PT and this effect can be related to the mass transport, once the XRD patterns for the sintered samples did not present any difference of its correspondent calcined powders, except the absence of PbO_2 extra peak in PL2 sample. The pore sealing at the initial stage of sintering is very important to avoid PbO volatilization, because it could harm the densification process. The enhancement in the mass transport helps the pore sealing and consequently reduces the weight loss from 3.0 wt% for pure sample to 2.6 wt% for PL1 and PL2 samples.

The effects of lithium doping in ceramic microstructure can be observed by SEM images (Fig. 3). The most important microstructural effect for high amount of lithium, markedly for PL2 sample, is the tendency of transgranular fractures originated from PbO segregation. During the sintering process, the PbO_2 phase originated from charge compensation of negatively charged Li'_{Mg} sites in PL2 powder sample is decomposed in PbO phase, enhancing the mechanical resistance of the grain boundaries. As consequence, the grain boundaries become mechanically stronger than the perovskite grains and lead to the occurrence of transgranular fractures in this sample. The presence of this PbO layer in PL2 ceramic sample, besides the enhancement of the mass transport caused by lithium addition, as observed by the more agglomeration degree in PL2 powder sample, should lead to the increasing in densification and grain growth effects. However, in spite of the slightly grain growth verified for PL2 ceramic sample, the ceramic density staying unaltered in ~7.8 g/cm^3 and no alteration in the porosity was also observed. The probable cause for this occurrence is the more agglomeration degree in PL2 powder sample, which makes more difficult the powder compaction stage and attenuate the densification process.

The curves of dielectric constant and dielectric loss as function of temperature at the frequency of 1 kHz for 0.9PMN–0.1PT ceramics are shown in Fig. 4. K_m value increases from 18,000 to 20,000 when 1 mol% of lithium is added to the pure composition, and for 2 mol% of lithium, K_m goes to 21,000. It was determined that the dielectric loss has no significant variation and the dielectric constant around T_m is not proportional to lithium content. The lower T_m value

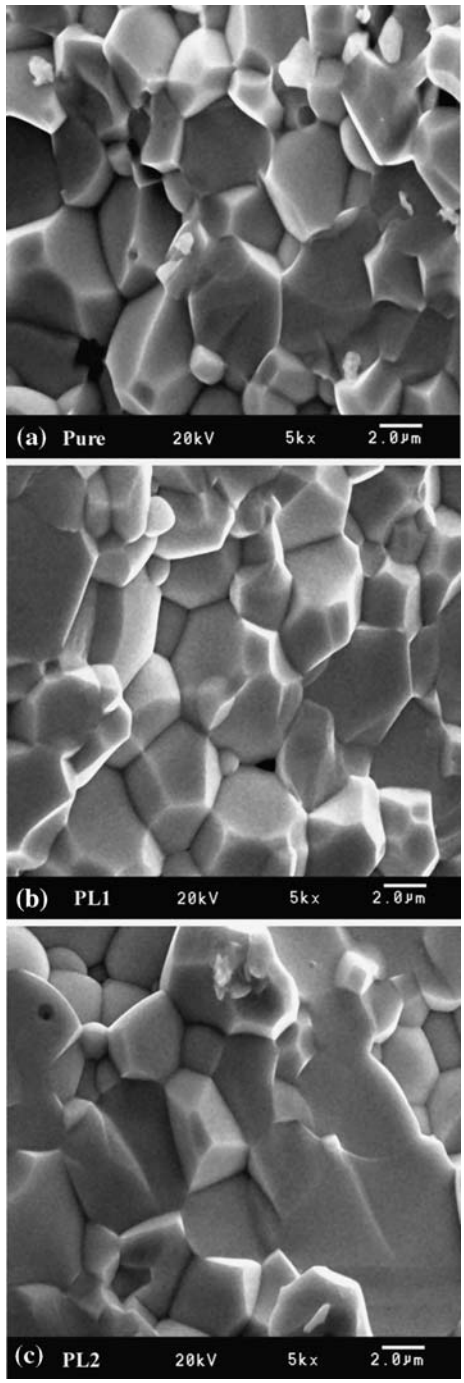

Fig. 3 SEM images of 0.9PMN–0.1PT sintered ceramics (**a**) pure, (**b**) PL1, and (**c**) PL2

presented for PL2 compared to PL1 sample can be consequence of the accentuated Pb deficiency in the perovskite phase, what makes the grain weaker than grain boundary and generates the observed transgranular fracture for this sample. Comparatively, when potassium is added directly in the A site [18], T_m also decreases and the relaxor character is enhanced as a

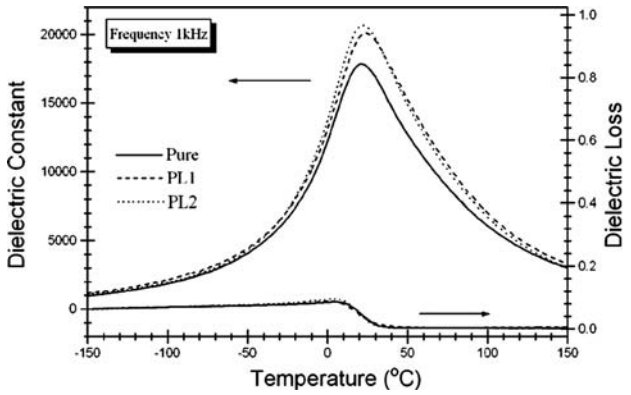

Fig. 4 Dielectric constant and dielectric loss as function of temperature for pure, PL1 and PL2 ceramic samples

direct consequence of PbO deficiency in the perovskite structure.

The diffusiveness parameter (δ), calculated as described elsewhere [18], showed a decreasing for doped samples, from 41.6 °C for pure sample to 40.0 and 38.1 °C for PL1 and PL2 samples, respectively. As discussed in previous work [13], lithium enhances the columbite crystallinity, which is associated to a more chemically ordered structure. Thus, the diffusiveness of phase transition is reduced as consequence of the minor randomness of B cations.

In Fig. 5 is shown the dependence between T_m and K_m values as function of electric-field frequency (ω) for all samples. The increasing of K_m value is directly associated to the polarity of $B''O_6$ octahedron, which enhances when the difference between x coordinates for B and oxygen cation (Δx) increases (Table 1). In other words, the dipole moment increases when the center between positive and negative charges moves

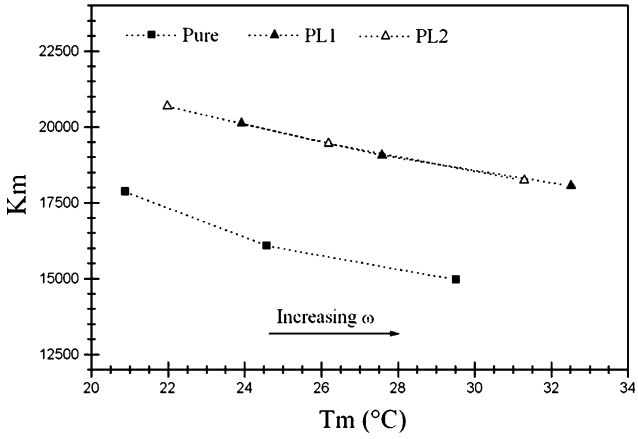

Fig. 5 K_m and T_m values as function of electric-field frequency for 0.9PMN–0.1PT ceramics

away of the cell center. Different from pure sample, the curves of PL1 and PL2 samples perform a common curve, in spite of the displacement of individual points. This means that a correspondent variation between T_m and K_m is verified so that the increasing in the polarity of $B''O_6$ octahedron is followed by an increasing in cations thermal agitation in the perovskite structure, responsible for the decreasing in T_m, possibly due to a more amount of Pb and O vacancies in PL2 sample. The generated oxygen vacancy in the same B random site, in which lithium is added, can accentuate the polarity of the neighbor $B''O_6$ octahedron, which causes the additional increase in K_m value for PL2 sample, despite the reduction in Δx value for this sample.

The ΔT_m values, obtained from the difference between T_m values at 1 and 100 kHz, provide an indication of the relaxor behavior for these samples. It was found that relaxor behavior increases from 8.5 °C (pure and PL1 samples) to 9.5 °C (PL2 sample). It is known that the relaxor behavior is enhanced by the reduction of the ferroelectric/anti-ferroeletric (FE/AFE) coupling. The FE/AFE coupling can be altered either by changes in the FE behavior, which increases with the molar volume, or by changes in AFE behavior, which increases with the ionic radii difference between B′ and B″ cations [19]. When lithium substitutes magnesium in B′ site, the AFE behavior increases due the increasing in the difference of ionic radii between the cations of B′ and B″ cations. However, for PL1 sample, a proportional increasing in molar volume is also verified (lattice parameter increasing), responsible by the enhancement in the FE behavior. It results in no variation for FE/AFE coupling compared to the pure sample, as verified by the same ΔT_m values.

For PL2 sample, the increasing in lithium concentration does have a correspondent increase in molar volume, while the difference between the ionic radii stays increasing. Thus, there is an increasing in the AFE behavior but there is not in the FE behavior, causing the enhancement in the relaxor behavior. These results can be corroborated by observing the P vs. E curves in Fig. 6. The ferroelectric behavior is always characterized by a hysteresis loop in the P vs. E curve, which is gradually lost when the anti-ferroelectric behavior is increased. Different from pure and PL1 samples, which exhibit a hysteresis loop with a remanent polarization of ~1 $\mu C/cm^2$, PL2 sample does not present any hysteresis loop, and consequently, zero of remanent polarization, proving that the addition of 2 mol% of lithium enhances the relaxor behavior in 0.9PMN–0.1PT system.

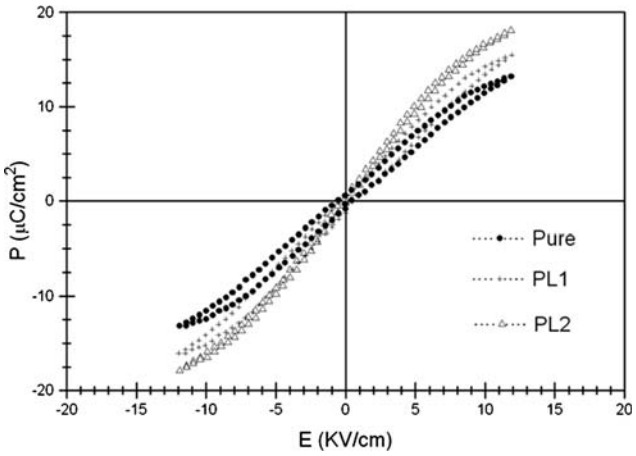

Fig. 6 Polarization (P) vs. electric-field (E) curves for 0.9PMN–0.1PT ceramic samples

Conclusions

The Ti-modified columbite route has shown to be an efficient method to synthesize pyrochlore-free 0.9PMN–0.1PT powders. A satisfactory mechanism for relatively low-level substitutions of lithium in the ceramic has been suggested. The substitution of Li^{+} ions for Mg^{2+} ions in the B-site sub-lattice of the perovskite generates Pb and O vacancies for the ionic compensation of negatively charged Li'_{Mg} sites. When lithium concentration is increased from 1 to 2 mol%, the perovskite structure becomes Pb deficient and the mass transport is enhanced. It leads to more agglomerated powders and grain boundary mechanically stronger than the grain in the sintered ceramic. The addition of 2 mol% of lithium increases K_m values and enhances the relaxor behavior as consequence of an increasing in anti-ferroelectric characteristics.

Acknowledgements The authors thank FAPESP and Capes Brazilian agencies for the financial support.

References

1. Pastor XM, Bajpai PK, Choudhary RNP (2005) Bull Mater Sci 28(3):199
2. Chen YH, Uchino K, Shen M, Viehland D (2001) J Appl Phys Soc 90(3):1455
3. Koval V, Briancin J (2003) Ceram Silik 47(1):8
4. Yimnirun R, Ananta S, Meechoowas E, Wongsaenmai S (2003) Phys D: Appl Phys 36(13):1615
5. Takesue N, Fuji Y, You H (2002) Ferroelectr 270:1335
6. Zhang R, Peng S, Xido D, Wang Y, Yang B, Zhu J, Yu P, Zhang W (1998) Cryst Res Techol 33(5):827
7. Gu H, Shih WY, Shih W-H (2003) J Am Ceram Soc 86(2):217
8. Swartz SL, Shrout TR (1982) Mat Res Bull 17:1245
9. Bouquin O, Lejeune M, Boilot JP (1991) J Am Ceram Soc 74(5):1152
10. Ring TA (1996) Fundamentals of ceramic powder processing and synthesis. Academic, San Diego, USA
11. Bruno JC, Cavalheiro AA, Zaghete MA, Cilense M, Varela JA (2004) Mater Chem Phys 84(1):120
12. Cavalheiro AA, Zaghete MA, Cilense M, Villegas M, Fernández JF, Varela JA (2004) Bol Esp Ceram Vídrio 43(3):653
13. Bruno JC, Cavalheiro AA, Zaghete MA, Cilense M, Varela JA (2005) Mater Sci Forum 498–499:642
14. Shannon RD (1976) Acta Crys A32:751
15. Fanning DM, Robinson IK, Jung ST, Colla EV, Viehland DD, Payne DA (2000) J Appl Phys 87(2):840
16. Lee K-M, Janga HM (1997) J Mater Res 12(6):1614
17. Che J, Yao X (2004) Ceram Int 30:1377
18. Bruno JC, Cavalheiro AA, Zaghete MA, Varela JA (2006) Ceram Int 32(2):189
19. Zhang QM, You H, Mulvihill ML, Jang SJ (1996) Solid State Commun 97(8):693